EURASIP Journal on Applied Signal Processing 2005:16, 2686–2693
© 2005 Hindawi Publishing Corporation

# DSP-Enabled Radio Astronomy: Towards IIIZW35 Reconquest

**Rodolphe Weber**
*Laboratoire d'Electronique, Signaux, Images, Polytech'Orleans, Université d'Orléans, 12 rue de Blois, BP 6744, 45067 Orléans Cedex 2, France*
*Email: rodolphe.weber@univ-orleans.fr*

**Cédric Viou**
*Station de Radioastronomie de Nançay, Observatoire de Paris, CNRS No. 704, 18330 Nançay, France*
*Email: cerdric.dumez-viou@obs-nancay.fr*

**Andrée Coffre**
*Station de Radioastronomie de Nançay, Observatoire de Paris, CNRS No. 704, 18330 Nançay, France*
*Email: andree.coffre@obs-nancay.fr*

**Laurent Denis**
*Station de Radioastronomie de Nançay, Observatoire de Paris, CNRS No. 704, 18330 Nançay, France*
*Email: laurent.denis@obs-nancay.fr*

**Philippe Zarka**
*LESIA, Observatoire de Paris, CNRS, 5 Place Jules Janssen, 92195 Meudon, France*
*Email: philippe.zarka@obspm.fr*

**Alain Lecacheux**
*LESIA, Observatoire de Paris, CNRS, 5 Place Jules Janssen, 92195 Meudon, France*
*Email: alain.lecacheux@obspm.fr*

*Received 31 January 2004; Revised 24 February 2005*

In radio astronomy, the radio spectrum is used to detect weak emission from celestial sources. By spectral averaging, observation noise is reduced and weak sources can be detected. However, more and more observations are polluted by man-made radio frequency interferences (RFI). The impact of these RFIs on power spectral measurement ranges from total saturation to subtle distortions of the data. To some extent, elimination of artefacts can be achieved by blanking polluted channels in real time. With this aim in view, a complete real-time digital system has been implemented on a set of FPGA and DSP. The current functionalities of the digital system have high dynamic range of 70 dB, bandwidth selection facilities ranging from 875 kHz to 14 MHz, high spectral resolution through a polyphase filter bank with up to 8192 channels with 49 152 coefficients and real-time time-frequency blanking with a robust threshold detector. This receiver has been used to reobserve the IIIWZ35 astronomical source which has been scrambled by a strong satellite RFI for several years.

**Keywords and phrases:** digital receiver, filter banks, real-time detection, radio astronomy.

## 1. INTRODUCTION

Radio astronomy, in common with many other users of the radio spectrum, has the advantage of a few protected frequency bands. However, most scientific questions find their answers in unprotected bands where radio astronomy is not a primary user. Moreover, even in the protected bands, out-of-band emission regulations are not always sufficient to prevent the pollution of astronomical primary bands. As a result, an increasing number of observations become unusable (see Figure 1d).

In practice, the signals received from astronomical objects are considered as correlated Gaussian noise. From the power spectral shape, some astrophysical information, such

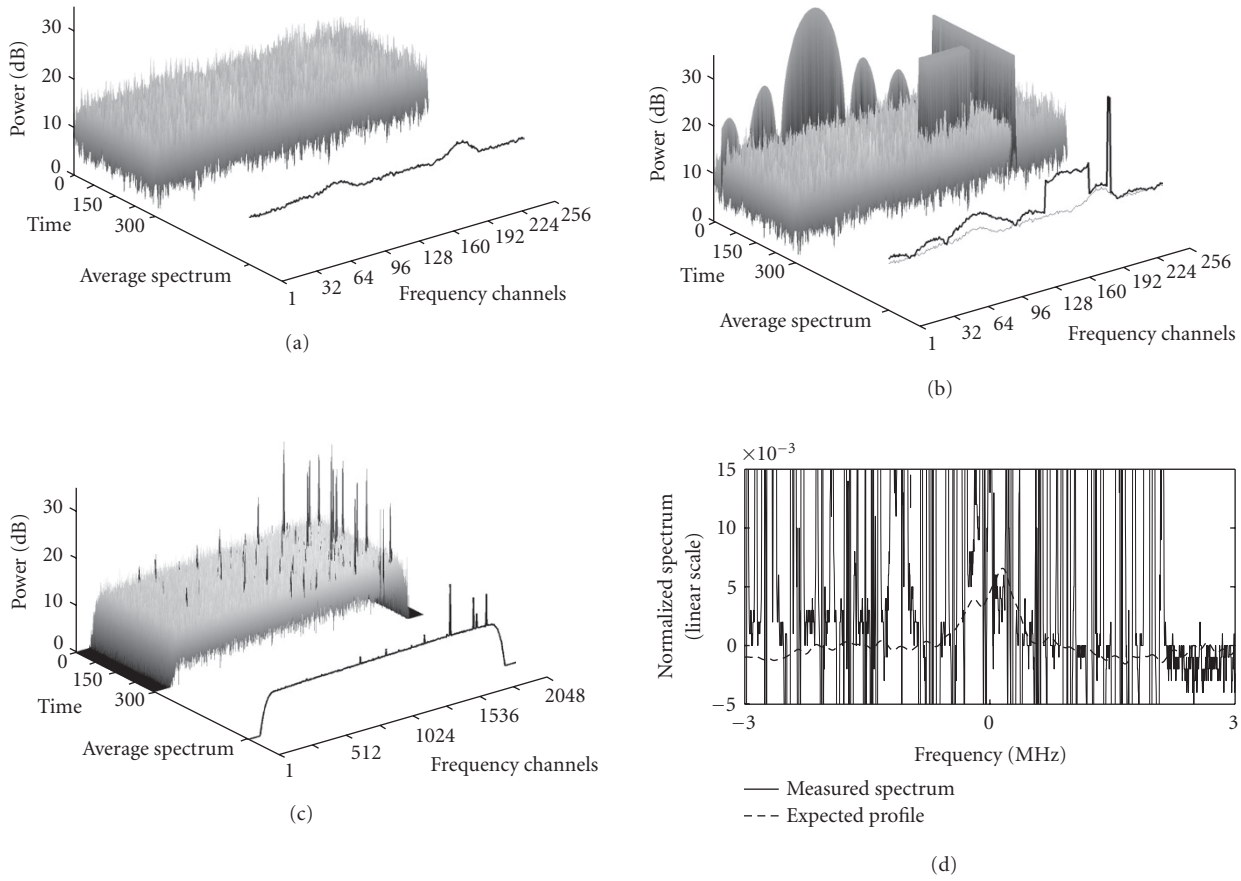


Figure 1: Examples of time-frequency planes. (a) The synthesized signal of interest (SOI) is buried in the system noise, a power spectral averaging must be done to make the SOI profile visible (solid line). (b) The same SOI with several synthesized RFIs: (i) wideband RFI, (ii) time-frequency located RFI, (iii) continuous frequency line. The averaged power spectrum is distorted. (c) Real SOI corrupted with RFI from a LEO. (d) Zoom on the expected power spectra of the real SOI and what is really measured: observations are not possible.

as, the existence of an astronomical object, its mass, its red shift, and its rotation speed, are extracted. Depending on the radio telescope sensitivity, the signal of interest (SOI) to system noise ratio is generally around −50 dB. However, source detection can still be done by averaging the power spectral information over a time $\tau$ (see Figure 1a). If any RFI emission occurs during this averaging time, the whole power spectral estimation is corrupted (see Figures 1b and 1c), unless a fine time-frequency blanking of the input signal is applied prior to the averaging. In this case, the time-frequency slots detected as polluted are removed so that only free time-frequency slots will be averaged.

The first point is to ensure that time-frequency slots free from interferences still exist between corrupted ones. Recent radio spectrum experimental surveys [1, 2] have shown that with 1 millisecond by 1 kHz time-frequency slots, efficient discrimination of most RFIs can be achieved. However, in some specific bands, optimal time-frequency slots may be narrower than a few hundred Hertz or shorter than a few microseconds (radar case). In any case, to recover these potential RFI free time-frequency slots, the digital receiver must have some kind of time and frequency agility.

Another point is that the signal of interest (SOI) can be completely buried in the system noise. Furthermore, RFI levels can have very large fluctuations due to propagation and moving effects. For example, it is common to measure RFI to system noise ratio varying from insignificant to more than 60 dB. However, contrary to the field of telecommunication, this problem cannot be overcome by an automatic gain control because of its negative impact on both sensitivity and calibration issues. On one hand, the least significant bit must be preserved throughout the processing to keep the astronomical information available and, on the other hand, a high dynamic range must also be achieved to prevent any saturation due to RFI.

Unfortunately, classical receivers were not designed to operate in such conditions. First, their poor dynamic range spreads the RFI over the whole spectrum. Secondly, the analog filters used in such systems do not provide enough frequency selectivity. Thirdly, their spectral resolution and channel selectivity are often too limited to extract the free channels from the corrupted ones. Finally, their hardware architecture is too specific to allow additional functions, such as RFI detection, to be implemented. With this aim in view,

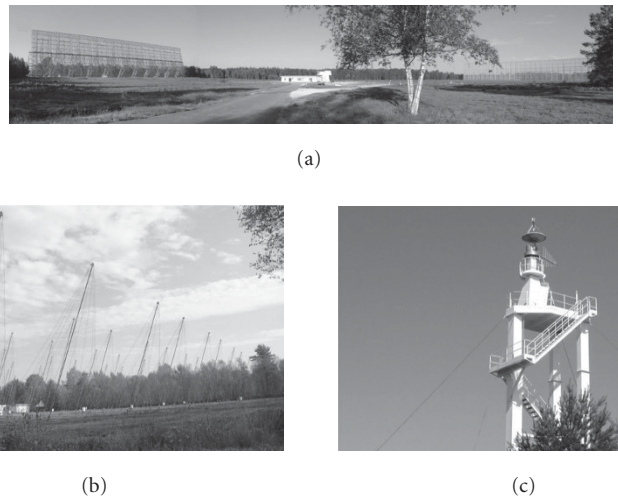

(a)

(b)

(c)

Figure 2: (a) *The decimeter radio telescope* covers the frequency band between 10 MHz and 90 MHz with two polarizations. In this band, the sky noise is predominant, so that mainly high-level radio sources such as the Sun or Jupiter can be observed. The RFI environment is quite nonstationary due to ionosphere effects. To achieve efficient blanking, high frequency resolution down to few hundred Hertz is needed. (b) *The decameter radio telescope* covers the frequency band between 1 GHZ to 4 GHz with two polarizations. In this band, sky noise is very low. Thus, the measured signal (if no RFI) is dominated by system noise. Depending on the RFI, different time and frequency resolutions are needed. (c) *The surveillance antenna* covers the frequency band between 10 MHz to 4 GHz. An automatic RFI survey is done with a classical spectrum analyzer, but finer spectral analysis can be done with the digital receiver presented in this paper.

a new generation of digital receivers, with "software-defined radio" capabilities, has been recently designed [3, 4, 5, 6]. These receivers differ from one another by their specifications such as the input bandwidth, the number of bits, the number of channels, or other more specific parameters.

In this paper, the design of a robust and multipurpose radio astronomy receiver is presented. It has been specifically designed for the Nançay Observatory's single-dish telescopes (France). Two radio telescopes and a surveillance antenna are currently connected to this receiver (cf. Figure 2). First, the overall architecture is given in Section 2. Then, the band selection implementation is detailed in Section 3. The high-resolution digital filter banks are described in Section 4. Finally, recent results of a real-time RFI detection algorithm implemented in the receiver and applied on actual observations are shown in Section 5.

## 2. ROBUST RECEIVER ARCHITECTURE

Figure 3 describes the global architecture of the robust receiver (RR). It can drive simultaneously 8 signals (RF) coming from the different radio telescopes. Each RF signal is independently downconverted to an intermediate frequency (IF) of 70 MHz, providing a final usable bandwidth of 14 MHz. These 8 IF signals are simultaneously digitized and processed by 8 banks consisting of digital modules plugged on PCI boards (HEPC9 and HERON modules from Hunt Engineering). Each of these banks includes a 14-bit ADC (analog device), 1 FPGA VIRTEX II 1000 (Xilinx), 1 FPGA VIRTEX II 3000 (Xilinx) with 256 Mb external RAM and 2 DSP TMS320C6203 (Texas Instruments). An industrial PC is used to drive 2 banks with data exchange capabilities. The four necessary PCs are connected via a fast Ethernet link to a central computer for further data analysis, compression, and storage.

To increase the observational flexibilities of the receiver, a switch matrix has been included in the analog downconverter process. Depending on its configuration, any of the 8 RF inputs can be redirected to one or more of the 8 IF bands. In particular, several subbands (contiguous or not) from the same RF input can be processed in several digital banks running the same or different algorithms. For example, one bank can make a coarse analysis of the signal in order to detect some specific event. If detection occurs, it will trigger a fine analysis of the same signal on a second bank. Such an application is under development at Nançay Observatory to perform automatic detection and storage of Jovian bursts.

The primary function of the RR is to provide high-resolution spectral analysis. This functionality has been implemented in the two FPGAs (see the following sections), leaving DSPs still available for post-detection RFI mitigation techniques (see an example in Section 5).

## 3. BAND SELECTION IMPLEMENTATION

The global process is given in Figure 4. From the 14 MHz bandwidth of the IF, a frequency bandwidth between 14 MHz and 875 kHz is digitally downconverted to baseband. Downconversion is performed digitally in two steps. First, undersampling is applied with a 56 MHz sampling clock. Then, a direct digital synthesizer (DDS) followed by successive decimation filters selects the band of interest.

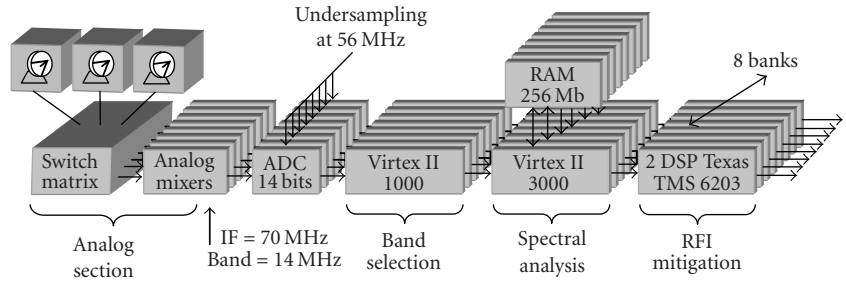


Figure 3: Overview of the robust receiver. The flow can be reconfigured to share the calculation power between all the banks.

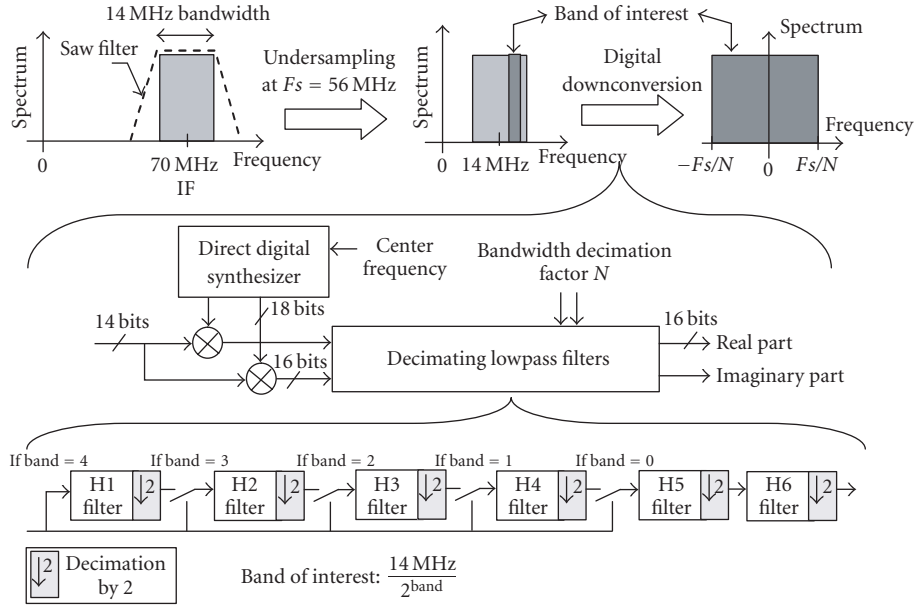


Figure 4: Overview of digital downconversion and band selection process. The 14 MHz usable bandwidth is centerd at 70 MHz. The antialiasing filter is a saw filter, which offers a better frequency rejection (70 dB). The bandwidth is selected between 875 kHz to 14 MHz through a set of filters $Hi, i = 1, \ldots, 6$. The filter characteristics are given in Table 1. The output signal is a baseband complex signal coded with 16 bits. This design fits into an FPGA, VIRTEX II 1000 (Xilinx). The system clock is 56 MHz.

The DDS is a lookup table which contains the values of a sine wave coded with 18 bits. Two multipliers are used to produce the real and imaginary parts of the mixed signal. The DDS system clock is 56 MHz.

The decimation filters have been optimized both to minimize the logic resources and to maximize the frequency selectivity. Thus, five half-band filters have been implemented to process the bandwidth selection. Given that half of their coefficients are null, their implementation can be resource-efficiently achieved by polyphase realization [7]. A final selective FIR filter with 83 coefficients completes the processing. At each filtering step, the dataflow can be decimated by two. The aliasing is limited by an efficient filter frequency selectivity which yields to a final frequency rejection of 75 dB. In terms of hardware implementation, with a good use of half-band properties, coefficient redundancy, polyphase structures, and resource sharing, a reduction of the hardware resources required is possible (see Table 1).

Finally, only 38 multipliers are used for the whole implementation of the DDC. This design has been fitted into an FPGA VIRTEX II 1000 (Xilinx). The input flow is 56 MHz with 14 bits real data, and the maximum output flow is 14 MHz with 16 bits complex data. The next step is the spectral analysis.

## 4. SPECTRAL ANALYSIS IMPLEMENTATION

The spectral analysis has two functions. The first one is to provide spectral information on the SOI for radio astronomers. The second one is to make a segmentation of the time-frequency plane with a view of performing the best RFI blanking. High dynamic range considerations are still present at this stage.

In practice, given the large flow of data to be processed, classical radio telescope receivers use correlators that coarsely quantize spectra in time, which generally allows RFI excision

Table 1: The decimating lowpass filters. The input and output signals of each filter are coded with 16 bits. Without any design optimization, the implementation requires 226 multipliers. With design optimizations (polyphase structures, coefficient redundancy, and resource sharing between real and imaginary parts), only 36 multipliers are needed. Their system clock is 56 MHz.

| Filter name | H1 | H2 | H3 | H4 | H5 | H6 |
|---|---|---|---|---|---|---|
| Type | Half-band | Half-band | Half-band | Half-band | Half-band | FIR |
| Filter order | 6 | 6 | 10 | 10 | 18 | 82 |
| Normalized cutoff frequency | 0.5 − 1/128 | 0.5 − 1/64 | 0.5 − 1/32 | 0.5 − 1/16 | 0.5 − 1/8 | 1/4 |
| Attenuation (dB) | 119 | 95 | 100 | 77 | 81 | 75 |
| Number of bits for the coefficients | 6 | 6 | 10 | 11 | 14 | 17 |
| Number of multipliers without optimization | 8 | 8 | 12 | 12 | 20 | 166 |
| Number of multipliers implemented | 2 | 2 | 3 | 3 | 5 | 21 |

only in the frequency domain. Some types of RFI are much more effectively removed from data with high time resolution so a system has been designed in which resolutions in the time and frequency domains can be chosen to suit the situation.

Depending on the RFI properties (see the next section), the time-frequency resolution must be reconfigured. Two methods have been designed for the FPGA VIRTEX II 3000 (Xilinx). In both cases, the output is a power spectrum coded with either 32 bits or 48 bits.

For high frequency selectivity, an 8192-bin polyphase filter bank [7] can be used (see Figure 5a). The impulse response of the lowpass filter model is 4 9152 samples long. Since no overlap is needed to maximize the sensitivity of the power spectra estimation, this filter bank is critically decimated. In Figure 5b, the performances in terms of frequency selectivity are compared with those obtained from equivalent weighted FFT. With this polyphase filter bank, the maximum frequency resolution is 107 Hz for an 875 kHz bandwidth.

For high time resolution, a 64-bin weighted FFT with 50% overlap can be downloaded in the FPGA. The maximum time resolution is then 2.29 microseconds for 14 MHz bandwidth but frequency resolution is only 218.79 kHz.

For an intermediate compromise between time and frequency resolution, the number of FFT bins can be extended up to 4096 with the same design.

Moreover, a parameterized scaling factor can be applied according to the RFI context. Indeed, the management of the dynamic is different depending on whether the filtered signal is pure noise (i.e., RFI free) or not. For the moment, this parameter is set by the operator, but it is planned to make it adaptative in the future.

Besides, a preintegration of the spectra can be done inside the FPGA. The output spectra are sent to the DSPs for disk storage or further processing such as RFI detection.

## 5. EXAMPLE OF REAL-TIME ROBUST DETECTION ALGORITHM

Various methods have been experimented to eliminate those RFI depending on the type of interferences and the type of instruments [8, 9, 10, 11]. The present study focuses on time-frequency blanking on data coming from a single dish.

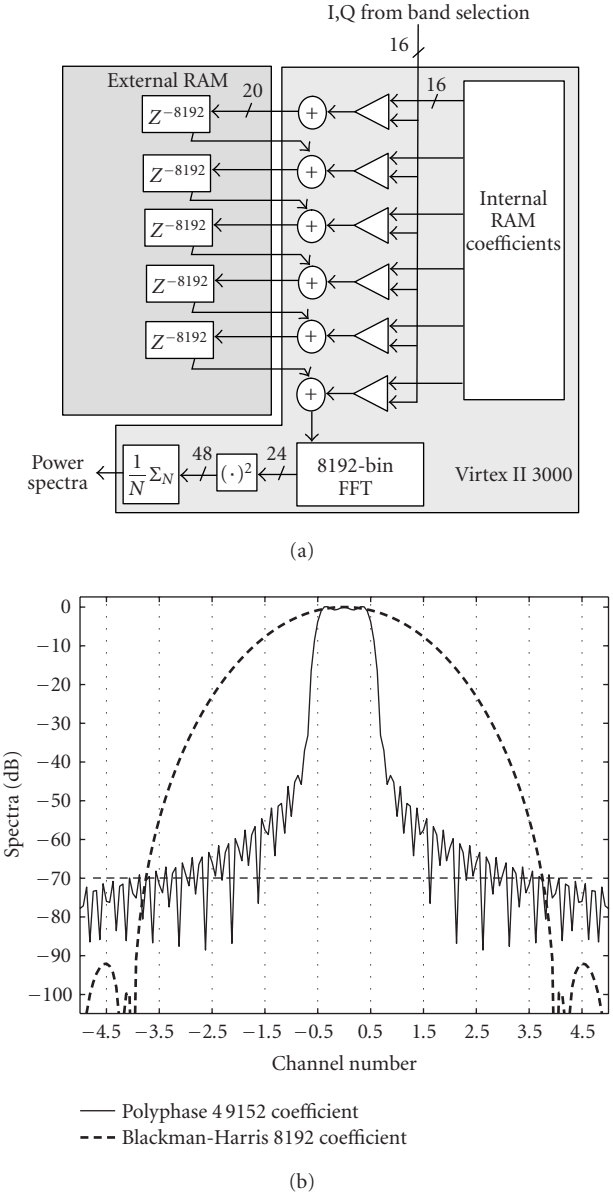


Figure 5: Polyphase filter bank process. (a) 8192-bin polyphase filter bank architecture. (b) Comparison of the spectral resolution and channel rejection between a Blackman-Harris windowing and a polyphase filter bank with 4 9152 coefficients.

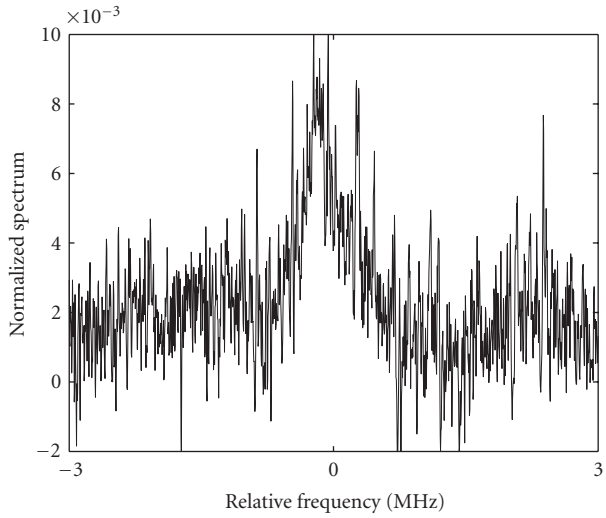


Figure 6: Time-frequency block blanking ($\Delta t = 1, \Delta f = 3$), blanking threshold $S = \mu_{Ho} + 9 \cdot \sigma_{Ho}$.

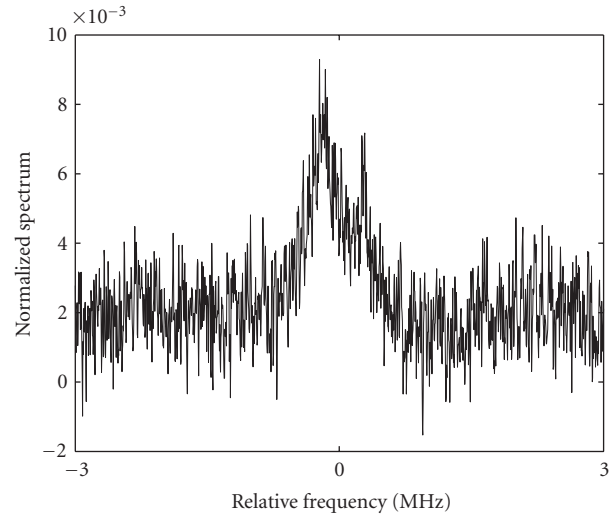


Figure 7: Time-frequency block blanking ($\Delta t = 1, \Delta f = 3$), blanking threshold $S = \mu_{Ho} + 4 \cdot \sigma_{Ho}$.

From the power time-frequency (T-F) plane generated in the previous processing step, we want to separate all the T-F points corrupted by an RFI (case named H1 hypothesis) from those which are not (case named H0 hypothesis).

The simple idea, which has been implemented, is to use a power criterion to perform this discrimination. Other criteria based on cyclostationary properties are also under study [12].

Under the H0 hypothesis, the measured signal is assumed to be an almost white Gaussian noise (i.e., the system noise is predominant). Thus, in the T-F plane, the threshold, $S$, corresponding to a given probability of false alarm, can be easily derived:

$$S = \mu_{H_0} + C \cdot \sigma_{H_0}, \tag{1}$$

where $C$ is a constant depending on the required discrimination rate, $\mu_{Ho}$ is the mean of the T-F distribution under the H0 hypothesis and $\sigma_{Ho}$ is the absolute distance of the T-F distribution under the H0 hypothesis. Absolute distance has been preferred to standard deviation because it is more robust to RFI and its implementation does not require multipliers. Given that the estimation of $\mu_{Ho}$ and $\sigma_{Ho}$ must use RFI free T-F points to guarantee the H0 hypothesis, robust estimators have been implemented.

Robust estimation can be done by median filtering or by exploiting some RFI properties. For example, if the RFI has narrowband properties, only a few frequency bins of the T-F plane are polluted at a given time. Besides, among these bins, only those with high power values may alter the estimation of $\mu_{Ho}$ and $\sigma_{Ho}$ under the H0 hypothesis. Thus, by discarding these extreme and easily detectable values, a robust estimation of $\mu_{Ho}$ and $\sigma_{Ho}$ can be computed.

This technique has been used on the decimeter radio telescope at Nançay to observe the mega maser IIIZW35 that is located in the band also used by a constellation of LEO (low earth orbit) telecommunication satellites. Their TDMA and FDMA modulations lead to RFI bursts spread in time and frequency (see Figure 1c). The source cannot be seen with traditional receivers (see Figure 1d).

In our experiment, the robust mean and absolute distances are estimated in real time as described previously. The number of frequency bins is 2048. A block $(\Delta t, \Delta f)$ of the T-F plane is blanked as soon as one of the T-F points inside the block exceeds the threshold. To compare the different blanking schemes, two complementary criteria are evaluated:

(i) loss of data which is the volume of data blanked over the whole volume of data,

(ii) pollution level which is the ratio between the standard deviation after blanking and the expected standard deviation under H0 hypothesis; perfect blanking has an ideal pollution level equal to one.

In this paper, two kinds of block patterns are compared with two kinds of threshold.

(i) *Time-frequency block blanking* ($\Delta t = 1, \Delta f = 3$). The size of this block matches the T-F location of the RFI bursts. Figure 6 gives the result for $C = 9$ and Figure 7 for $C = 4$. The false alarm probability corresponds, respectively, to 0.4% and 3.5%.

(ii) *Full spectrum blanking* ($\Delta t = 1, \Delta f = 2048$). The complete spectrum is blanked as soon as one channel exceeds the threshold. This kind of blanking can be useful when the RFI is suspected to have sidelobes that are difficult to detect. The counterpart is that the loss of data is considerable and may be unacceptable when the threshold is too low. This is the case with $C = 4$. Figure 8 shows the result for $C = 9$.

In the case of IIIZW35 polluted by these LEO satellites, the time-frequency block blanking method with $C = 4$ is a good compromise (i.e., the loss of data and the polluted level are minimized). The choice of $(\Delta t, \Delta f)$is completely dependent on the RFI context. For example, tests on radar

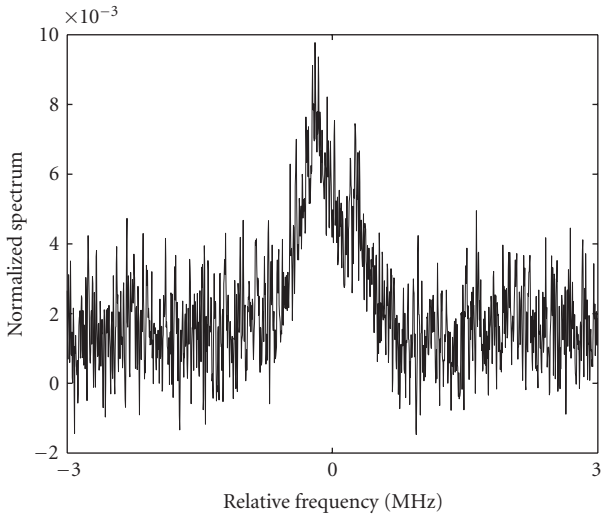


Figure 8: Full spectrum blanking ($\Delta t = 1$, $\Delta f = 2048$), blanking threshold $S = \mu_{Ho} + 9 \cdot \sigma_{Ho}$.

have shown that the full spectrum blanking is well suited to suppress this kind of broadband RFI. The choice of $C$ depends on the astronomical and scientific needs. If the observed source needs precise measurements, a low threshold must set. The sensitivity will decrease but the data will be very clean.

The algorithm has been implemented on a fixed point DSP TMS320C6203 (Texas Instruments). The DSP/BIOS runs 3 tasks: reading raw spectra from the FPGA chain, handling the blanking, and writing processed spectra toward the host PC. The code was optimized to speed up the calculation. The system was configured to record 2048 bins spectra of 7 MHz bandwidth at a rate of 584 microseconds. This time resolution is obtained with an integration of 8 spectra done in the FPGA before detection.

## 6. CONCLUSIONS

In this paper, the digital implementation of a new generation of radio astronomical receivers has been presented. The robustness of our system towards RFI is provided by improved linearity, higher frequency rejection, and better spectral resolution compared to current receiver designs. Thus, the signal integrity can be preserved and real-time RFI mitigation techniques can be envisaged. Our system is fully reconfigurable and can be adapted to any RFI context. With a simple but robust algorithm, a radio astronomical source that has been unobservable for several years has been rediscovered. Now, the key points are the implementation of other efficient RFI mitigation algorithms and the improvement of receiver characteristics such as bandwidth. These developments are essential for the next generation of radio telescopes such as the frequency agile solar radio telescope (FASR) or the square kilometer array (SKA).

## ACKNOWLEDGMENTS

The authors gratefully acknowledge people who have made the reconquest of IIIZW35 possible: L. Amiaud, D. Aubry, L. Bacquart (ALSE), P. Colom, C. Fabrice, E. Gérard, E. Jolivet, J.M. Martin, P. Renaud, and C. Rosolen. The Nançay Radio Observatory is the Unité Scientifique de Nançay of the Observatoire de Paris, associated as Unité de Service et de Recherche No. 704 to the Centre Nationale de la Recherche Scientifique (CNRS). The Nançay Observatory also gratefully acknowledges the financial support of the Conseil Régional de la Région Centre, France. The work of C. Viou was financially supported by Observatoire de Paris and by the European Social Fund.

## REFERENCES

[1] V. Clerc, *Implémentation de processus hétérogènes de traitement du signal en temps réel à contrainte moyenne. Application à la radioastronomie*, Ph.D. thesis, University of Paris 6, Paris, France, February 2003.

[2] P. A. Fridman, "RFI mitigation with the time-frequency robust statistical analysis," in *Proc. IUCAF Summer School: Spectrum Management for Radio Astronomy*, National Radio Astronomy Observatory, Green Bank, WVa, USA, June 2002, http://www.iucaf.org/sschool/procs/.

[3] W. A. Baan, P. A. Fridman, and R. P. Millenaar, "RFI mitigation at WSRT: algorithms, test observations, system implementation," in *JFC session, XXVIIth General Assembly of the International Union of Radio Science*, Maastricht, the Netherlands, August 2002.

[4] M. R. W. Masheder, *AstroFFT: Astronomical Digital Spectrometer*, http://portal.beam.ltd.uk/products/astrofft/astrofft.html.

[5] M. Kramer, A. G. Lyne, B. C. Joshi, et al., "COBRA, a digital receiver at Jodrell Bank," in *Proc. IUCAF RFI Mitigation Workshop*, Bonn, Germany, March 2001.

[6] C. Rosolen, V. Clerc, and A. Lecacheux, "High dynamic range, interference tolerant, digital receivers for Radio Astronomy," *The Radio Science Bulletin*, no. 291, pp. 6–12, 1999.

[7] P. P. Vaidyanathan, *Multirate Systems and Filter Banks*, Signal Processing Series, Prentice Hall, Englewoods Cliffs, NJ, USA, 1993.

[8] A. Leshem and A.-J. van der Veen, "Multichannel interference mitigation techniques in radio astronomy," *Astrophys. J. Suppl. S.*, vol. 131, no. 1, pp. 355–373, 2000.

[9] C. Barnbaum and R. F. Bradley, "A new approach to interference excision in radio astronomy: real-time adaptive cancellation," *Astron. J.*, vol. 116, no. 5, pp. 2598–2614, 1998.

[10] S. W. Ellingson, J. D. Bunton, and J. F. Bell, "Removal of the GLONASS C/A signal from OH spectral line observations using a parametric modeling technique," *Astrophys. J. Suppl. S.*, vol. 135, no. 1, pp. 87–93, 2001.

[11] P. A. Fridman and W. A. Baan, "RFI mitigation methods in radio astronomy," *Astronomy & Astrophysics*, vol. 378, no. 1, pp. 327–344, 2001.

[12] S. Bretteil and R. Weber, "Comparison between two cyclostationary detectors for RFI mitigation in radio astronomy," in *Proc. 12th European Signal Processing Conference (EUSIPCO '04)*, Vienna, Austria, September 2004.

**Rodolphe Weber** was born in Tunisia in 1967. He received the Engineering degree from École Nationale Supérieure de l'Electronique et de ses Applications, Cergy, France, in 1991. He received the Ph.D. degree from the University of Paris XI, Orsay, France, in 1996, for his work on radio frequency interference detection in radio astronomy. Since 1996, he has been working as a Teacher and Researcher at Polytech'Orléans, Orleans, France, in the field of high-speed digital electronics and signal processing. Besides, he is the Coordinator of the Nançay RFI Mitigation Group.

**Cédric Viou** graduated from École Supérieure des Procédés Electroniques et Optiques (University of Orléans, France). His majors were embedded systems and signal processing. He currently works at the Nançay Observatory as a Ph.D. student, developing and implementing algorithms for RFI mitigation.

**Andrée Coffre** has been working as a Software Engineer for 20 years at Nançay Observatory. She writes on either real-time software for computers controlling various radio telescopes of the observatory or dedicated postprocessing software in high-level languages.

**Laurent Denis** has been working as an Electronic Engineer for 20 years at Nançay Observatory. He built many radioastronomy receivers, starting with classical heterodyne system and is now moving to digital ones.

**Philippe Zarka** is a Research Scientist at LESIA (Laboratory for Space Studies and Instrumentation in Astrophysics), Paris Observatory, CNRS. He works and teaches in the fields of radioastronomy (ground-based and space-borne instruments), and planetary and explanatory physics.

**Alain Lecacheux** is a Research Scientist at LESIA (Laboratory for Space Studies and Instrumentation in Astrophysics), Paris Observatory, CNRS. He works in the fields of radioastronomy, planetary physics, and high-energy cosmic rays.